



Original paper

Development of a dose distribution shifter to fit inside the collimator of a Boron Neutron Capture Therapy irradiation system to treat superficial tumours

N. Hu^{a,b,*}, H. Tanaka^b, S. Yoshikawa^a, M. Miyao^c, K. Akita^a, T. Aihara^a, K. Ono^a

^a Osaka Medical College, Kansai BNCT Medical Center, Osaka, Japan

^b Kyoto University, Institute for Integrated Radiation and Nuclear Science, Osaka, Japan

^c Osaka Medical College Hospital, Central Department of Radiology, Osaka, Japan



ARTICLE INFO

Keywords:

BNCT
Neutron moderator
Thermal neutrons
Bolus
Monte Carlo simulation

ABSTRACT

The Kansai BNCT Medical Center has a cyclotron based epithermal neutron source for clinical Boron Neutron Capture Therapy. The system accelerates a proton to an energy of 30 MeV which strikes a beryllium target producing fast neutrons which are moderated down to epithermal neutrons for BNCT use. While clinical studies in the past have shown BNCT to be highly effective for malignant melanoma of the skin, to apply BNCT for superficial lesions using this system it is necessary to shift the thermal neutron distribution so that the maximum dose occurs near the surface. A dose distribution shifter was designed to fit inside the collimator to further moderate the neutrons to increase the surface dose and reduce the dose to the underlying normal tissue. Pure polyethylene was selected, and a Monte Carlo simulation was performed to determine the optimum thickness of the polyethylene slab. Compared with the original neutron beam, the shifter increased the thermal neutron flux at the skin by approximately 4 times. The measured and simulated central axis depth distribution and off axis distribution of the thermal neutron flux were found to be in good agreement. Compared with a 2 cm thick water equivalent bolus, a 26% increase in the thermal neutron flux at the surface was obtained, which would reduce the treatment time by approximately 29%. The DDS is a safe, simple and an effective tool for the treatment of superficial tumours for BNCT if an initially fast neutron beam requires moderation to maximise the thermal neutron flux at the tissue surface.

1. Introduction

Boron neutron capture therapy (BNCT) is a binary treatment modality that consists of two separate components to achieve its therapeutic effect. It is based on the nuclear reaction that occurs when a thermal neutron is captured by a ^{10}B atom, producing high LET particles. The ranges of these high LET particles (alpha particle and ^7Li nuclei) are approximately 10 μm and 4 μm in tissue, respectively, which is on the order of the size of a melanoma cell [1]. Currently, the majority of BNCT treatments conducted worldwide use neutrons generated from a nuclear reactor. However, the trend is to consider an accelerator-based neutron system to promote BNCT as a standard treatment technique in cancer therapy, as the system needs to be one that can be easily installed and safely operated in a hospital environment. This has motivated the

development of accelerator-based neutron sources and there are already several countries that have developed or are currently developing the system for application in BNCT [2].

The accelerator system installed in the Kansai BNCT Medical Center at the Osaka Medical College utilises a 30 MeV proton beam with a beryllium target generating neutrons with an energy of up to 28 MeV. The produced neutrons traverse through a moderator material which slows the neutrons down to the epithermal energy range. The system is designed such that the peak of the thermal neutron flux occurs at a depth of approximately 2 cm from the skin surface, making it suitable for tumours seated several centimetres below the skin surface [3]. Clinical interest in BNCT has focused primarily on high grade gliomas [4,5] and patients with recurrent tumours of the head and neck region [6–10]. Currently, the two clinically available tumour seeking ^{10}B compounds

* Corresponding author at: Osaka Medical College, Kansai BNCT Medical Center and Kyoto University, Institute for Integrated Radiation and Nuclear Science, Osaka-fu Takatsuki-shi Daigakumachi 2-7, Japan

E-mail address: ko.naonori.7z@kyoto-u.ac.jp (N. Hu).

<https://doi.org/10.1016/j.ejmp.2021.01.003>

Received 3 May 2020; Received in revised form 20 December 2020; Accepted 6 January 2021

Available online 4 February 2021

1120-1797/© 2021 Associazione Italiana di Fisica Medica. Published by Elsevier Ltd. This is an open access article under the CC BY-NC-ND license

(<http://creativecommons.org/licenses/by-nc-nd/4.0/>).

are BSH ($\text{Na}_2\text{B}_{12}\text{H}_{11}\text{SH}$) and ^{10}B -p-boronphenylalanine (BPA). The latter, which is a boronated amino acid and is taken up into tumour cells due to increased amino acid transport, is more commonly used. Mishima first proposed the use of BNCT for melanoma utilising the specific melanin synthesis activity of melanoma cells [11]. Later in 1988, Mishima applied BNCT for malignant melanoma using the thermal neutron irradiation mode at the Kyoto University research reactor [12]. Fukuda performed an analysis on the research performed by Mishima and the results indicated an increase in CR (complete response) with BNCT compared with X-ray radiotherapy [13]. In 2003, a phase I/II clinical trial for treating cutaneous melanomas with BNCT was performed in Argentina [14]. This study showed complete response in 21 of 25 cases treated indicating a promising result.

To perform BNCT for superficial tumours using this system, the thermal neutron distribution needs to be adjusted to produce maximum thermal neutron flux at the skin surface, resulting in high absorbed dose to tumour at the skin surface. One method is to utilise a bolus material (as in conventional radiotherapy) to provide a build-up effect [15,16]. However, there are some difficulties with the use of bolus for BNCT, such as

1. Commercially available bolus (commonly used for high energy electron radiotherapy) is made up of a mixture of elements which may emit unwanted prompt gamma rays after being irradiated by neutrons (or becomes radioactive).
2. Patient orientation during BNCT is unique and the patient set-up is not always simple. Placing a bolus over the treatment area may not be easily achieved.
3. In some cases, placing bolus over the skin increases the source to skin distance, which results in a decrease of neutron flux, which ultimately increases the treatment time.

To overcome these issues, a dose distribution shifter (DDS) to fit inside the collimator opening was investigated.

2. Methods

2.1. Evaluation of an optimum material

The material for the DDS was evaluated using a Monte Carlo simulation package called Particle and Heavy Ion Transport code System (PHITS). PHITS can transport most particle species with energies up to 1 TeV by using several nuclear reaction models and data libraries. Neutron induced nuclear reactions were simulated using Japanese Evaluated Nuclear Data Library (JENDL 4.0) [17]. Material with high hydrogen content is commonly used to moderate fast neutrons. A list of materials considered for the DDS in this study are shown in Table 1. These materials were selected based on low cost and ease of manufacturing. The thickness of each material was increased by 0.5 cm increments and the thermal neutron flux at the surface was evaluated using PHITS. The material which produced the largest number of thermal neutrons at the phantom surface was selected and the thermal neutron, epithermal neutron, fast neutron, and gamma ray fluxes at the beam exit were simulated for various thicknesses (Fig. 1). The relative standard errors for all PHITS Monte Carlo simulation were less than 0.5%, unless stated otherwise.

Table 1
List of materials considered for the DDS.

Material	Density (g/cm^3)	Chemical formula
Water	1	H_2O
Acrylic	1.18	$\text{C}_5\text{O}_2\text{H}_8$
Polyethylene	0.94	C_2H_4

2.2. Phantom experiment

A 2 cm thick cylindrical plate made from pure polyethylene was manufactured for all four collimator sizes (10 cm, 12 cm, 15 cm, and 25 cm diameter). The thermal neutron flux distribution inside a water phantom was evaluated using gold foil activation method, described in the appendix. Gold wire (weight percent 99.95%) of 0.25 mm diameter and cadmium pipe of 0.5 mm thickness were used in the measurement of thermal neutron flux.

A thermo-luminescent dosimeter (TLD) of BeO enclosed in a quartz glass capsule was used in the measurement of gamma ray dose rate. The BeO TLD has little sensitivity to low energy neutrons. Sakurai et al. measured the thermal neutron sensitivity of this TLD at the Kyoto University Research Reactor [18]. This study showed a thermal neutron fluence of $8 \times 10^{12} \text{n}/\text{cm}^2$ resulted in approximately 1 cGy gamma-ray dose. The thermal neutron fluence at each TLD position was determined using gold foils to correct for the thermal neutron sensitivity. The gold wire and TLDs were placed along the central beam axis to measure the distribution along the beam axis, shown in Fig. 2. Gold wires were also placed 2.5 cm and 5 cm in the lateral direction from the centre to measure the off-axis thermal neutron flux distribution.

2.3. Comparison to a water equivalent bolus set up

A 2 cm thick $15 \times 15 \text{ cm}^2$ water bolus was simulated to be sandwiched between the water phantom and the collimator (Fig. 3). The thermal neutron flux and the total RBE weighted dose, which is the summation of the four distinct radiation components (boron dose, gamma ray dose, nitrogen dose, neutron dose (see appendix)) were calculated and compared with the DDS system. The ^{10}B concentration in the phantom (healthy tissue) was assumed to be $25 \mu\text{g}/\text{g}$ and the relative biological effectiveness (RBE) for nitrogen, hydrogen and gamma rays were also assumed to be 3.0, 3.0 and 1.0, respectively. The phantom material was set to soft tissue (ICRU four component) which is composed of hydrogen, carbon, nitrogen, and oxygen with a weight fraction of 0.10, 0.11, 0.03 and 0.76, respectively. The compound biological effectiveness (CBE) for tumour and skin was assumed to be 4.0 and 2.5, respectively, and the tumour to healthy tissue ^{10}B ratio of 3.0. These values were taken from Tanaka et al. [19]. The irradiation time was determined by setting a point dose limit at the skin (i.e. surface of the phantom) to 15 Gy-eq.

2.4. Clinical situation

For BNCT treatment, to maximise the neutron flux at the tumour region, the distance from the collimator to the patient must be kept as short as possible. However, depending on the treatment area, this may not be easily achieved and a small air gap between the patient surface and the collimator is unavoidable, particularly for head and neck cancers. The effect of an air gap on the thermal neutron flux along the beam axis was simulated. The distance from the collimator to the skin surface was varied, along with a different combination of DDS thicknesses.

In addition, the 2D dose distribution inside a humanoid head phantom was simulated using the BNCT treatment planning system SERA (Simulation Environment for Radiotherapy Applications) [20]. A mock tumour volume of a recurrent head and neck carcinoma with skin invasion was simulated and the dose distribution inside the tumour was evaluated. A 2 cm DDS with a 10 mm air gap was compared with a 1 cm thick bolus. A 1 cm bolus was selected to provide a similar build-up effect. The irradiation time was kept the same for both.

3. Results

From the three materials, polyethylene was found to produce the largest number of thermal neutrons at the surface, as shown in Fig. 4. PHITS simulation showed a polyethylene slab with a thickness of 2 cm

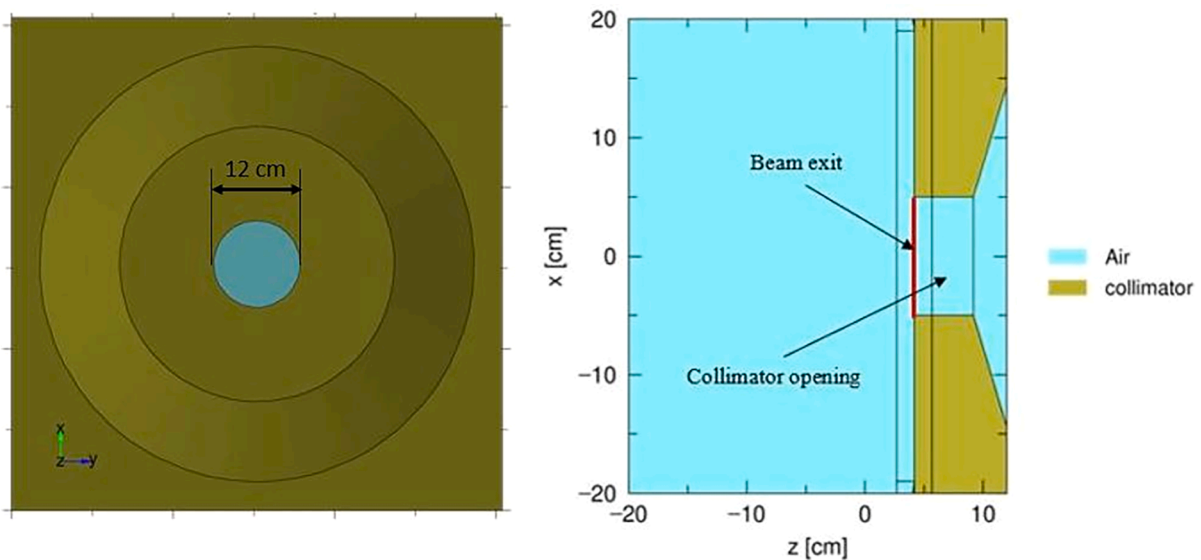


Fig. 1. Cross sectional geometry of the C-BENS collimator modelled using PHITS.

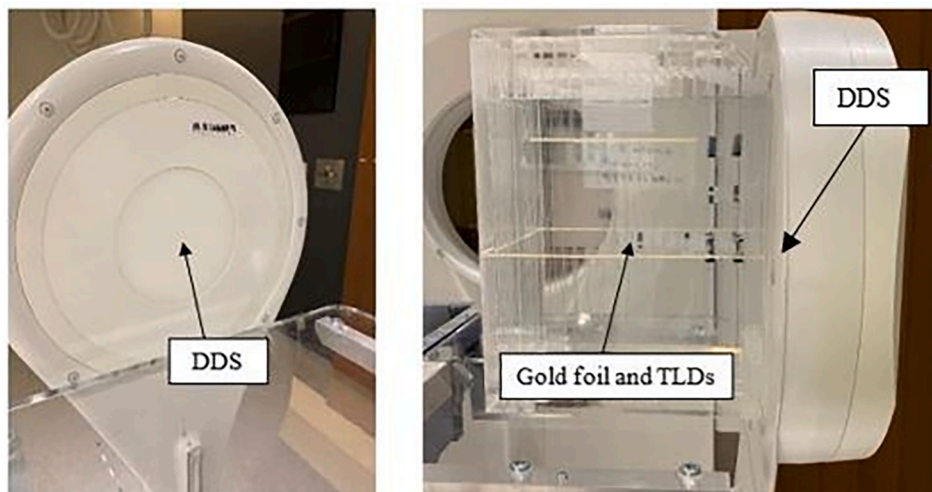


Fig. 2. Image of the experimental set up.

was found to produce the largest number of thermal neutrons at the surface and the corresponding neutron and gamma ray fluxes are shown in Fig. 5. The thermal neutron flux along the beam axis and off-axis for all four collimator sizes are shown in Figs. 6 and 7, respectively. The PHITS simulation showed a close agreement to measured values. The gamma ray dose rate along the beam axis for the 12 cm diameter DDS set up is shown in Fig. 8, also showed a close agreement between simulation and measured values. The central axis thermal neutron flux and gamma ray dose rate measurements were repeated 3 times and the average value was recorded. For the off-axis thermal neutron flux, measurement was only performed once due to time restriction on the machine.

The difference in the thermal neutron flux and the RBE weighted dose (for tumour cell and normal tissue) along the beam axis between the DDS and the bolus set up are shown in Figs. 9 and 10, respectively. The DDS had a 26% higher thermal neutron flux at the surface compared with the bolus setup. For a dose limit for the skin of 15 Gy-eq, the irradiation time for the DDS system was calculated to be 38 min and 49 min for the bolus set up. Due to the shorter treatment time with the DDS, the dose to the normal tissue was lower compared with the bolus treatment.

Fig. 11 shows the change in the thermal neutron flux along the beam axis as the gap between the collimator and the phantom surface was increased. As the gap was increased the peak position shifted a few millimetres into the water phantom. Table 2 shows the thermal neutron flux peak position for the various air gap and DDS thickness combination simulated using PHITS. Fig. 12 shows the 2D dose distribution of the tumour cell dose inside a humanoid phantom for a typical head and neck case. A 2 cm thick DDS with a 5 mm air gap showed a better dose coverage for a superficial tumour that has spread into the body. Fig. 13 shows the DVH of the tumour. For the same treatment time, the DDS showed a 20% increase at D90.

4. Discussion and conclusion

A dose distribution shifter designed to fit inside the collimator was developed and tested at the Kansai BNCT Medical Center. A cylindrical slab made from polyethylene with a thickness of 2 cm brought the maximum thermal neutron flux to the surface, making it suitable for superficial BNCT treatment (for e.g. malignant melanoma of the skin). Compared with water and acrylic, polyethylene produced the largest

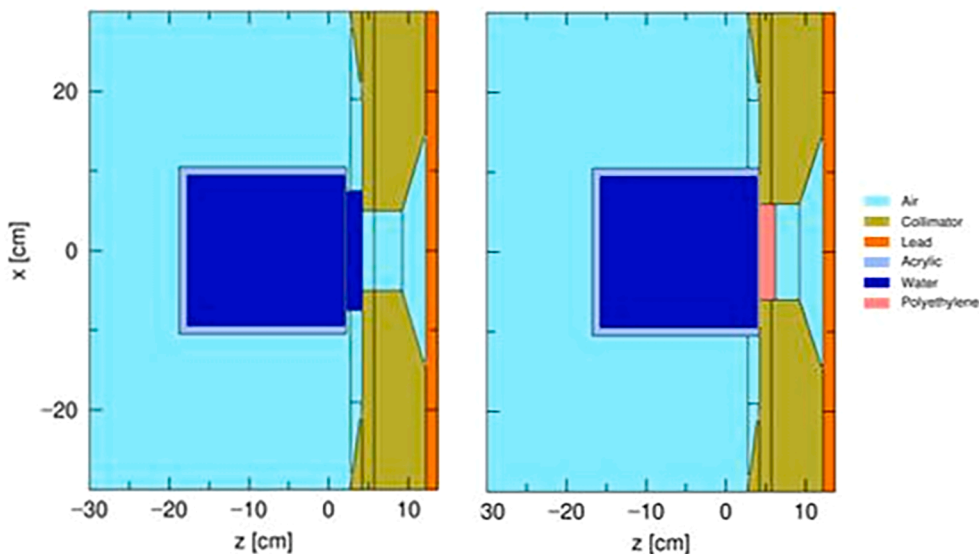


Fig. 3. Cross sectional image of the experimental set up modelled using PHITS of the bolus set (left) and the DDS set up (right).

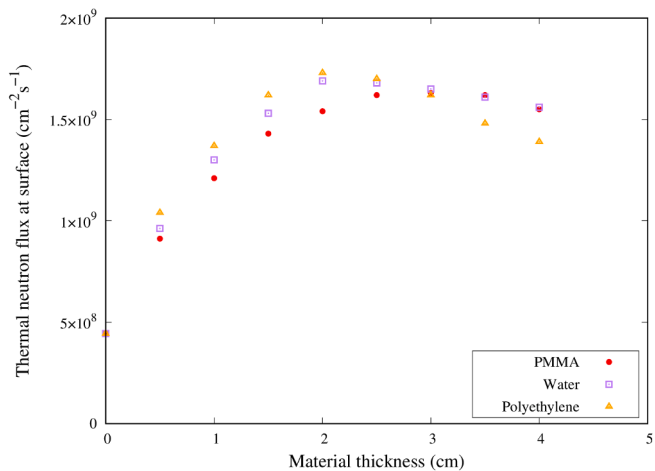


Fig. 4. Thermal neutron flux at the surface of the phantom for the different materials calculated using PHITS.

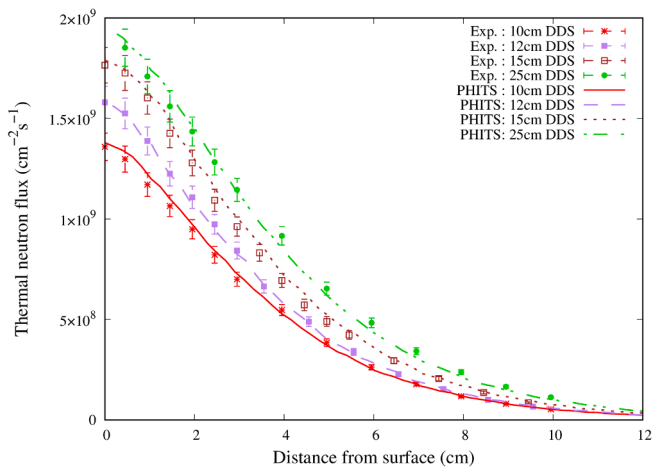


Fig. 6. Thermal neutron flux along the central beam axis inside a water phantom for the different collimator sizes.

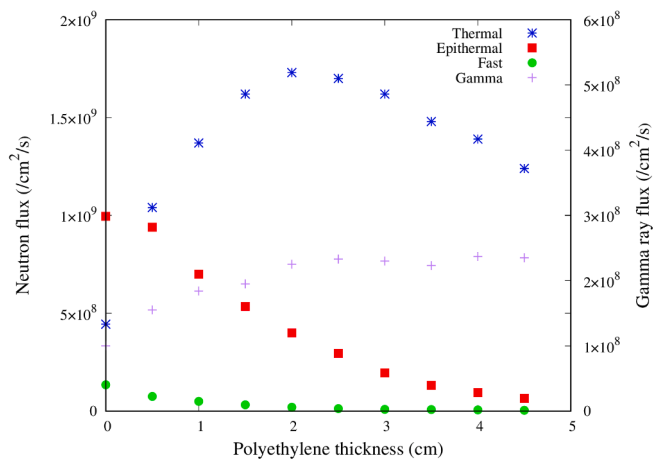


Fig. 5. Neutron and gamma ray flux at the beam exit as a function of polyethylene thickness calculated using PHITS.

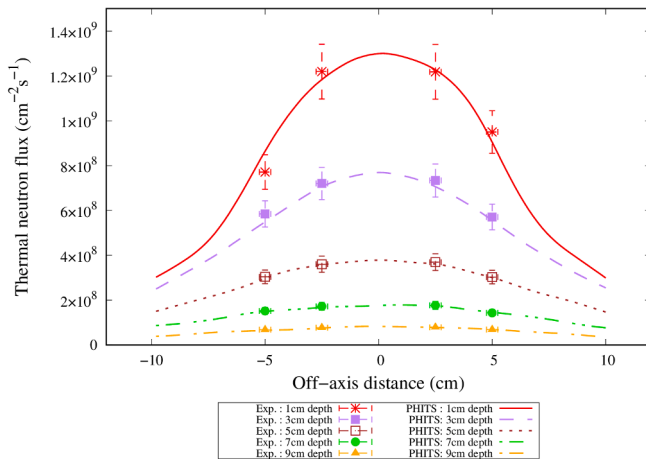


Fig. 7. Off-axis thermal neutron flux at several depths inside a water phantom for the 12 cm diameter DDS set up.

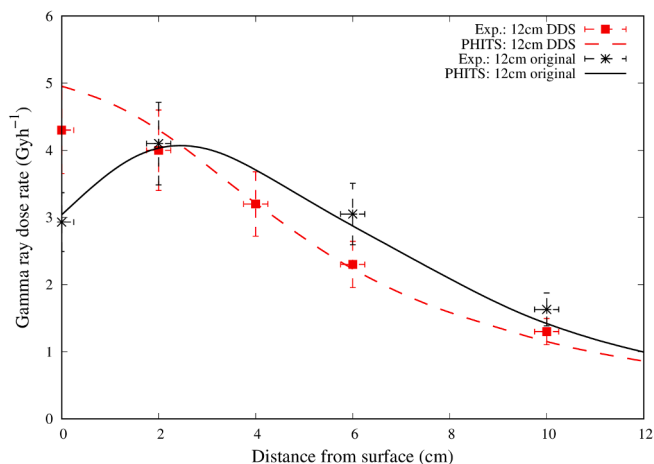


Fig. 8. Gamma ray dose rate along the beam axis inside a water phantom for the 12 cm diameter collimator with and without the DDS.

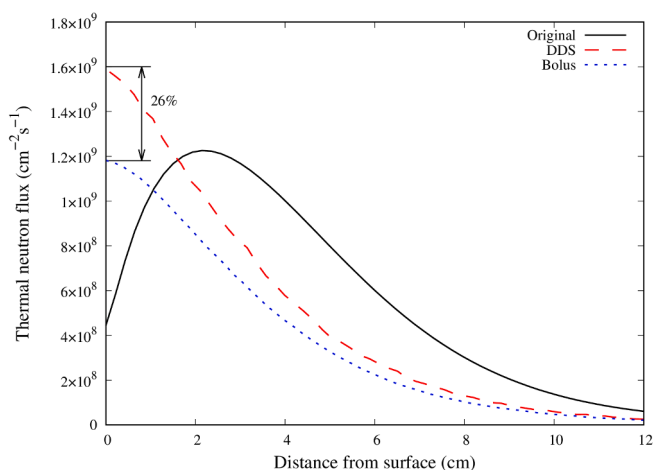


Fig. 9. Thermal neutron flux along the beam axis inside a water phantom for the 12 cm diameter collimator simulated with PHITS.

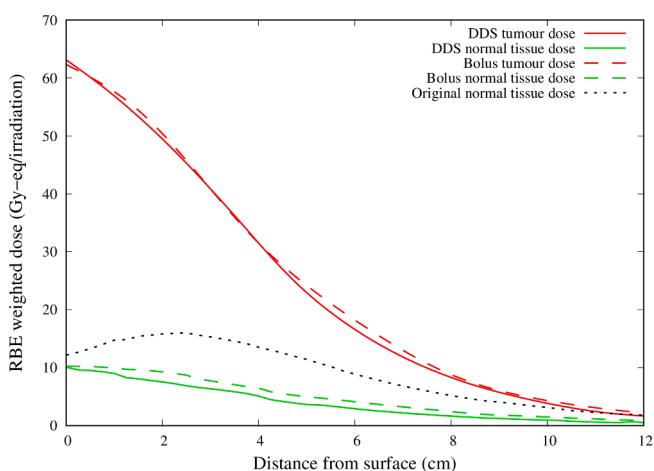


Fig. 10. RBE weighted dose along the beam axis for the 12 cm diameter collimator for a dose limit of 15 Gy-eq at the phantom surface (i.e. skin) with a tumour to normal tissue ratio of 3.0. The treatment time for the DDS was calculated to be 38 min and 49 min for the bolus setup.

number of thermal neutrons at the phantom surface. Polyethylene has a higher toughness compared to acrylic (maximum value of 220 J/m² for polyethylene and 25 J/m² for acrylic, determined from the Izod impact test [21]), which makes it less vulnerable to cracks during the manufacturing process. Also, future work will involve generating a more optimum shape suited for the patient, so a tough material which can withstand fine machining would be more suitable. Water is a cheap and readily available resource. However, water becomes activated by (n,p) reactions on oxygen for neutron energies above 10 MeV and handling of unsealed radioactive sources is troublesome. For the above reasons, polyethylene was selected as the material for the DDS. However, the disadvantage of polyethylene is the higher proportion of 2.2 MeV gamma rays produced from the hydrogen capture reaction. The PHITS simulation result showed a 12 cm diameter cylindrical polyethylene slab with a thickness of 2 cm produced approximately 30% more 2.2 MeV gamma rays compared with water. However, majority of gamma rays are produced from either inside the patient’s body (through neutron scattering processes) or from the primary beam itself, so this increase in the gamma ray was only a small fraction of the total gamma ray produced and resulted in a clinically insignificant change to the total dose delivered to the patient.

The effect of an air gap between the collimator surface and the phantom surface was also investigated. As the air gap was increased the thermal neutron flux peak position shifted a few millimetres into the phantom. This phenomenon may be due to the low energy thermal neutrons scattering in air and not reaching the phantom surface, resulting in a higher portion of higher energy thermal neutrons entering the phantom, producing a slight build-up effect. In a clinical situation, depending on the treatment region, it is not always possible to bring the patient surface flush onto the collimator surface. So hence, a thicker DDS (i.e. 3 cm) is necessary to bring the thermal neutron flux peak to the surface when an air gap is present. On the other hand, a small build-up may be effective for the treatment of shallow seated tumours. In this case, either a thinner DDS or increasing the air gap, or a combination of the two may result in a more effective treatment. For example, a 2 cm thick DDS with an air gap of 10 mm produced a relatively flat thermal neutron flux from the surface to approximately 1 cm depth along the central axis. This would produce a uniform dose distribution up to 1 cm, making it preferable for tumours that have spread few millimetres into the skin.

The advantage of the DDS over the bolus is evident during the patient set up and treatment process. In conventional radiotherapy, the patient lies on the treatment couch in a supine position and the gantry rotates around the patient. In BNCT, the patient needs to move his or her body such that the treatment area is as close to the collimator as possible. Some treatment set ups require the patient to be sitting with their head tilted and/or rotated for the duration of the treatment. Depending on the dose prescription, the treatment time may take up to an hour. Including the patient set up time, the total time can take up to 2 h. Placing the bolus onto the patient and making sure it is in the correct position and making sure it does not fall off during treatment adds even more time. The DDS is a simple system, where once the patient is aligned the DDS is placed into the collimator opening just before treatment, minimising the setup time. The DDS was found to reduce the irradiation time by approximately 29%, compared with a 2 cm bolus. This system would not only reduce the treatment time but may also reduce the patient set up time. Secondly, the DDS can be easily manufactured, with an accuracy of ± 0.1 mm. The thickness can be adjusted in the order of a millimetre, allowing for a better dose optimisation. This level of fine adjustment cannot be performed with a bolus. The third advantage of the DDS is the ability to treat several millimetres beyond the surface by generating a small gap between the DDS and the patient surface. The depth of a stage four melanoma may extend beyond 4 mm from the surface of the skin [22]. The DDS system has the flexibility to optimise the dose to the deeper region by either changing the thickness or producing an air gap between the DDS and the patient surface.

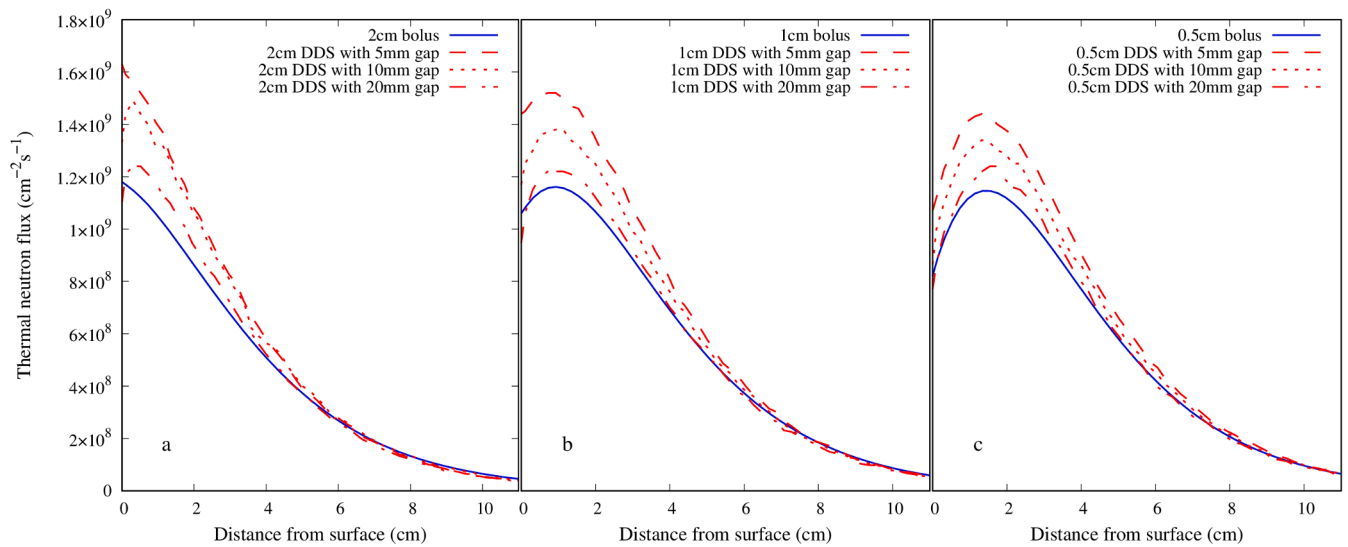


Fig. 11. Central axis thermal neutron flux of (a) 2 cm bolus and 2 cm DDS with varying air gap, (b) 1 cm bolus and 1 cm DDS with varying air gap, (c) 0.5 cm bolus and 0.5 cm DDS with varying air gap.

Table 2

Peak thermal neutron flux position for a combination of various air gap and DDS thickness simulated using PHITS.

DDS thickness (cm)	Peak thermal neutron flux position (cm) [± 0.21 mm]				
	No gap	5 mm gap	10 mm gap	15 mm gap	20 mm gap
0.5	1.47	1.47	1.47	1.47	1.47
1	0.84	1.05	1.05	1.26	1.26
2	0	0.21	0.42	0.42	0.63
3	0	0	0	0	0.42

dose to the healthy tissue surrounding the tumour region within the radiation field. A bolus can be moulded and shaped into the tumour region, allowing a better dose sparing of the healthy tissue surrounding the tumour. In a case where a tumour region is small and the smallest collimator aperture covers more healthy tissue than the tumour, a bolus may be more suitable than the current DDS. Another advantage of the bolus is the fact that an extra beam model is not required for the treatment planning process.

In the future, patient specific DDS may be created using a 3D printer to generate a negative of the patient surface segmentation from the CT images to optimise the treatment plan and the set-up time even more.

However, a uniform thickness and shape of the DDS may increase the

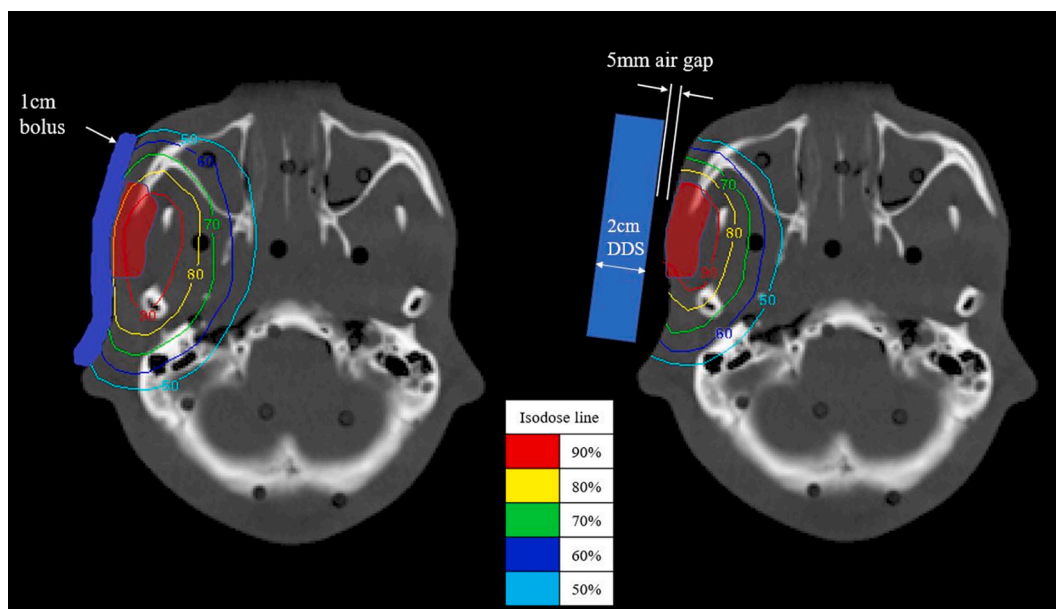


Fig. 12. 2D tumour cell dose distribution inside a humanoid phantom simulated using SERA for 1 cm bolus (left) and 2 cm DDS (right) with a 5 mm air gap. The red region indicates the tumour. (For interpretation of the references to colour in this figure legend, the reader is referred to the web version of this article.)

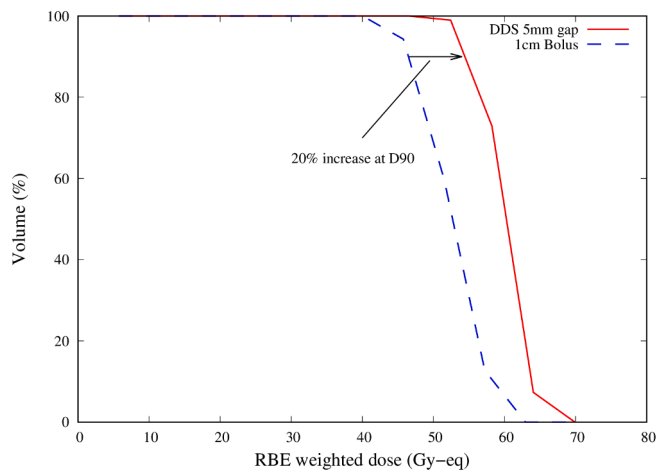


Fig. 13. Dose volume histogram of a mock tumour of a head and neck carcinoma with skin invasion. The treatment time was kept the same.

Appendix A

Gold foil activation method

A common detector for characterising BNCT beams is activation foils. Gold is commonly used for measuring both the thermal and epithermal neutron flux, as recommended by the IAEA TecDoc 1223 [23]. To distinguish between the thermal and epithermal neutron fluxes, measurements were performed both with bare and cadmium covered gold. Following neutron irradiation, the reaction rate of the gold sample is calculated using the expression below.

$$R = \frac{\lambda C}{\epsilon \gamma e^{-\lambda T_c} (1 - e^{-\lambda T_m}) \sum_{i=1}^n \left(\frac{Q_i}{\Delta t} (1 - e^{-\lambda \Delta t}) e^{-\lambda(n-i)\Delta t} \right)}$$

where ϵ is the detection efficiency of the detector of the gamma rays emitted from ^{198}Au , γ is the gamma ray emission rate from ^{198}Au decay, λ is the decay constant of ^{198}Au , T_c is the time from the irradiation to the start of the measurement, T_m is the measurement time, C is the peak count due to the detector measured gamma rays emitted from ^{198}Au and Q_i is the electric charge irradiated on the target at each interval, Δt .

BNCT dose component

The total dose delivered to a patient receiving BNCT is calculated by multiplying the absorbed dose of each radiation component present in the field with the corresponding RBEs and taking the sum.

$$D_T = CBE \times D_B + RBE_p \times D_p + RBE_n \times D_n + RBE_\gamma \times D_\gamma$$

where D_T represents the total absorbed dose from each component, described below.

The boron dose (D_B) is dose due to the ^{10}B fission reaction, $^{10}\text{B}(n, \alpha)^7\text{Li}$. The emitted alpha particle and the recoiling ^7Li ion result in locally deposited energy averaging about 2.33 MeV. The nitrogen dose (D_p) is the dose due to the ^{14}N in tissue capturing a thermal neutron and emitting a proton in a $^{14}\text{C}(n, \alpha)^{14}\text{N}$ reaction. The neutron dose (D_n) is the dose due to the epithermal and fast neutrons causing recoil protons from hydrogen in tissue. The gamma ray dose (D_γ) is the dose due to the gamma rays accompanying the neutron beam as well as gamma rays induced in the tissue itself. RBE_p , RBE_n and RBE_γ are RBE values of nitrogen, neutron, and gamma rays, respectively. CBE (compound biological effectiveness) considers the boron distribution inside a cell and is dependent on the boron compound type and the type of tissue being evaluated.

References

- [1] Luo Xi, Mitra D, Sullivan R, Wittner B, Kimura A, Pan S, et al. Isolation and molecular characterization of circulating melanoma cells. *Cell Rep* 2014;7(3): 645–53. <https://doi.org/10.1016/j.celrep.2014.03.039>.
- [2] Kreiner AJ, Bergueiro J, Cartelli D, Baldo M, Castell W, Asoia JG, et al. Present status of accelerator-based BNCT. *Reports Pract Oncol Radiother* 2016;21(2): 95–101. <https://doi.org/10.1016/j.rpor.2014.11.004>.
- [3] Tanaka H, Sakurai Y, Suzuki M, Masunaga S, Mitsumoto T, Fujita K, et al. Experimental verification of beam characteristics for cyclotron-based epithermal neutron source (C-BENS). *Appl Radiat Isot* 2011;69(12):1642–5. <https://doi.org/10.1016/j.apradiso.2011.03.020>.
- [4] Busse PM, Harling OK, Palmer MR, Kiger WS, Kaplan J, Kaplan I, et al. A critical examination of the results from the Harvard-MIT NCT program phase I clinical trial of neutron capture therapy for intracranial disease. *J Neurooncol* 2003;62(1-2): 111–21. <https://doi.org/10.1007/BF02699938>.
- [5] Miyatake S-I, Kawabata S, Yokoyama K, Kuroiwa T, Michiue H, Sakurai Y, et al. Survival benefit of Boron neutron capture therapy for recurrent malignant gliomas. *J Neurooncol* 2009;91(2):199–206. <https://doi.org/10.1007/s11060-008-9699-x>.
- [6] Kankaanranta L, Saarilahti K, Mäkitie A, Välimäki P, Tenhunen M, Joensuu H. Boron neutron capture therapy (BNCT) followed by intensity modulated chemoradiotherapy as primary treatment of large head and neck cancer with intracranial involvement. *Radiother Oncol* 2011;99(1):98–9. <https://doi.org/10.1016/j.radonc.2011.02.008>.
- [7] Kankaanranta L, Seppälä T, Koivunoro H, Saarilahti K, Atula T, Collan J, et al. Boron neutron capture therapy in the treatment of locally recurrent head-and-neck cancer: final analysis of a phase I/II trial. *Int J Radiat Oncol* 2012;82(1):e67–75. <https://doi.org/10.1016/j.ijrobp.2010.09.057>.
- [8] Ariyoshi Y, Miyatake S-I, Kimura Y, Shimahara T, Kawabata S, Nagata K, et al. Boron neutron capture therapy using epithermal neutrons for recurrent cancer in

- the oral cavity and cervical lymph node metastasis. *Oncol Rep* 2007. <https://doi.org/10.3892/or.10.3892/or.18.4.861>.
- [9] Aihara T, Hiratsuka J, Morita N, Uno M, Sakurai Y, Maruhashi A, et al. First clinical case of boron neutron capture therapy for head and neck malignancies using 18F-BPA PET. *Head Neck* 2006;28(9):850–5. <https://doi.org/10.1002/hed.20418>.
- [10] Kato I, Ono K, Sakurai Y, Ohmae M, Maruhashi A, Imahori Y, et al. Effectiveness of BNCT for recurrent head and neck malignancies. *Appl Radiat Isot* 2004;61(5):1069–73. <https://doi.org/10.1016/j.apradiso.2004.05.059>.
- [11] Mishima Y. Neutron capture treatment of malignant melanoma using 10B-chlorpromazine. *Pigment Cell Res* 1973;1:215–21.
- [12] Mishima Y, Honda C, Ichihashi M, Obara H, Hiratsuka J, Fukuda H, et al. Treatment of malignant melanoma by single thermal neutron capture therapy with melanoma-seeking 10b-compound. *Lancet* 1989;334(8659):388–9. [https://doi.org/10.1016/S0140-6736\(89\)90567-9](https://doi.org/10.1016/S0140-6736(89)90567-9).
- [13] Fukuda H, Hiratsuka J, Kobayashi T, Sakurai Y, Yoshino K, Karashima H, et al. Boron neutron capture therapy (BNCT) for malignant melanoma with special reference to absorbed doses to the normal skin and tumor. *Australas Phys Eng Sci Med* 2003;26(3):97–103. <https://doi.org/10.1007/BF03178777>.
- [14] González SJ, Bonomi MR, Santa Cruz GA, Blaumann HR, Larriou OAC, Menéndez P, et al. First BNCT treatment of a skin melanoma in Argentina: dosimetric analysis and clinical outcome. *Appl Radiat Isot* 2004;61(5):1101–5. <https://doi.org/10.1016/j.apradiso.2004.05.060>.
- [15] Seppälä T, Collan J, Auterinen I, Serén T, Salli E, Kotiluoto P, et al. A dosimetric study on the use of bolus materials for treatment of superficial tumors with BNCT. *Appl Radiat Isot* 2004;61(5):787–91. <https://doi.org/10.1016/j.apradiso.2004.05.054>.
- [16] Hirose K, Arai K, Motoyanagi T, Harada T, Shimokomaki R, Kato T, et al. EP-1436: A newly designed water-equivalent bolus technique enables BNCT application to skin tumor. *Radiother Oncol* 2017;123:5766. [https://doi.org/10.1016/S0167-8140\(17\)31871-6](https://doi.org/10.1016/S0167-8140(17)31871-6).
- [17] Shibata K, Iwamoto O, Nakagawa T, Iwamoto N, Ichihara A, Kunieda S, et al. JENDL-4.0: a new library for nuclear science and engineering. *J Nucl Sci Technol* 2011;48(1):1–30. <https://doi.org/10.1080/18811248.2011.9711675>.
- [18] Sakurai Y, Kobayashi T. Characteristics of the KUR Heavy Water Neutron Irradiation Facility as a neutron irradiation field with variable energy spectra. *Nucl Instrum Methods Phys Res Sect A Accel Spectromet Detect Assoc Equip* 2000;453(3):569–96. [https://doi.org/10.1016/S0168-9002\(00\)00465-4](https://doi.org/10.1016/S0168-9002(00)00465-4).
- [19] Tanaka H, Sakurai Y, Suzuki M, Masunaga S, Kinashi Y, Kashino G, et al. Characteristics comparison between a cyclotron-based neutron source and KUR-HWNIF for boron neutron capture therapy. *Nucl Instruments Methods Phys Res Sect B Beam Interact with Mater Atoms* 2009;267(11):1970–7. <https://doi.org/10.1016/j.nimb.2009.03.095>.
- [20] Wheeler F, Wessol D, Wemple C, Albright C, Cohen M, Frandsen M, et al. SERA -An Advanced Treatment Planning System for Neutron Therapy. *Ineel/Con-99 1999: 00523*.
- [21] Izod G. Testing Brittleness of Steel. *Engineering* 1903;76:431–2.
- [22] Breslow A. Thickness, cross-sectional areas and depth of invasion in the prognosis of cutaneous melanoma. *Ann Surg* 1970;172(5):902–8. <https://doi.org/10.1097/0000658-197011000-00017>.
- [23] Rorer D, Wambersie G. Current Status of neutron capture therapy. *IAEA*, 2001:75–7.